Research Article Vol. 16, No. 1 / 1 Jan 2025 / Biomedical Optics Express 245
Biomedical Optics EXPRESS

Hyper-brain independent component analysis (HB-ICA): an approach for detecting inter-brain networks from fNIRS-hyperscanning data

HAILING LUO,[1] YUTONG CAI,[1] XIUYUN LIN,[2,3] AND LIAN DUAN[1,4,*]

[1]School of Psychology, Shenzhen University, Shenzhen, China
[2]Institute of Developmental Psychology, Faculty of Psychology, Beijing Normal University, Beijing, China
[3]Beijing Key Laboratory of Applied Experimental Psychology, Faculty of Psychology, Beijing Normal University, Beijing, China
[4]Shenzhen Key Laboratory of Affective and Social Neuroscience, Center for Brain Disorders and Cognitive Sciences, Shenzhen University, Shenzhen, China
*duan_lian@szu.edu.cn

Abstract: Functional near-infrared spectroscopy (fNIRS) -based hyperscanning is a popular new technology in the field of social neuroscience research. In recent years, studying human social interaction from the perspective of inter-brain networks has received increasing attention. In the present study, we proposed a new approach named the hyper-brain independent component analysis (HB-ICA) for detecting the inter-brain networks from fNIRS-hyperscanning data. HB-ICA is an ICA-based, data-driven method, and can be used to search the inter-brain networks of social interacting groups containing multiple participants. We validated the method by using both simulated data and in vivo fNIRS-hyperscanning data. The results showed that the HB-ICA had good performance in detecting the inter-brain networks in both simulation and in-vivo experiments. Our approach provided a promising tool for studying the neural mechanism of human social interactions.

1. Introduction

Over the last twenty years, psychological and neural interaction processes during various social circumstances have been investigated broadly among people from all walks of life due to the introduction of a great new technology named hyperscanning [1–7]. Hyperscanning allows two or more interacting people's brain activities to be simultaneously measured [1,6,8]. In contrast to the traditional single-person paradigms, hyperscanning is helpful for revealing the psychological interaction processes and the neural covariation characteristics in natural social interaction scenarios. Hyperscanning has also been applied to study the neural mechanisms of autistic spectrum disorder [9,10] and social anxiety disorders [11,12].

Functional near-infrared spectroscopy (fNIRS) is a fast-developing brain imaging technology. Compared with other hyperscanning modalities such as functional magnetic resonance imaging (fMRI) and electroencephalogram (EEG), fNIRS is insensitive to head motion, very comfortable, and close to daily-life social interaction scenarios such as cooperation, competition, discussion, tuition, dinner, parenting and so on. Moreover, fNIRS has relatively high temporal and spatial resolution, and the ability of cortex localization, therefore can measure the neural activity in those typical social brain regions such as the medial prefrontal cortex and the temporoparietal cortex, with satisfactory temporal details of the neural interaction traces. These unique advantages make fNIRS-hyperscanning a very popular researching approach in social neuroscience field.

An important discovery from the hyperscanning studies is the inter-brain synchronization (IBS) phenomenon. In the past decade, a variety of studies have revealed that during social interactions, the neural activity from the specific brain regions of two different individuals are temporally synchronized, i.e., the IBS [8,13–15]. IBS is believed to rise on the foundation of the social

#542554 https://doi.org/10.1364/BOE.542554
Journal © 2025 Received 17 Sep 2024; revised 2 Dec 2024; accepted 15 Dec 2024; published 20 Dec 2024

Biomedical Optics EXPRESS

information transfer and processing between interacting individuals, and reflect their mental processes during the interaction such as understanding, mentalizing, empathy and so on [16–18].

In recent years, studying human social interaction from the perspective of inter-brain networks has received increasing attentions. Some researchers proposed that the neural process of social information transfer and processing can be viewed and modeled as the coactivation or coupling of the neural networks consisting of both interactors [19,20]. Moreover, Duan et al. [21] proposed the multi-brain network analysis approach and further employed it to investigate the cooperation process of a nine-person team [22]. In addition, Yang et al. [23] further extended the existing hyperscanning paradigm to study inter-group interaction.

The traditional inter-brain network analysis mainly relies on calculating the wavelet transform coherence (WTC) between the blood oxygenation signals recorded with fNIRS-hyperscanning [4,8,24]. The WTC method can detect the temporal-frequency coupling between two brain areas, and then the network can be constructed by taking the different brain regions as the nodes and the IBS among them as the edges. This method is simple to understand but has several disadvantages in application. First, this method is not good at separating the possibly existing multiple networks. The social interaction may involve multiple inter-brain networks of different functions, and these networks may have different temporal and frequency characteristics. It will be difficult to choose adequate frequency bands to calculate the IBS from the WTC temporal-frequency graph. Second, it is difficult for this method to characterize the network's temporal dynamics because the classical IBS calculation will compress both the temporal and frequency dimensions of the WTC graph. The researchers have to take additional operations such as the windowing method to obtain the network's dynamics [13,25]. Third, this method is sensitive to the global physiological noise. When the participants are interacting, their physiological activities such as heartbeat and respiration may also be commonly modulated by the interaction process. If not well removed, these physiological components may cause false synchronization.

The present study proposed an alternative method to calculate the inter-brain networks, which is based on the independent component analysis (ICA). ICA is a blind source separation (BSS) algorithm. It can decompose the signals into a series of statistically independent source components. ICA is a powerful approach that has been widely used in fNIRS studies to separate single-brain networks [26], and its effectiveness and reliability has also been well established [27] . It can identify distinct brain networks with their temporal dynamics and spatial patterns, and can also effectively separate the noise-related components.

In the present study, we developed a new method named hyper-brain ICA (HB-ICA) to detect distinct inter-brain networks of multiple interacting participants. The method consists of several steps including hyper-brain data pooling, ICA decomposition and components identification, and can finally obtain the spatial patterns and corresponding time courses of the inter-brain networks. In the following section, we introduce the theory and algorithm of the HB-ICA method. Subsequently, we validated this method by using both computer-simulated data and in-vivo data.

2. Hyper-brain independent component analysis (HB-ICA) method

2.1. Hyper-brain data pooling

In the hyper-brain data pooling step, all participants' fNIRS-hyperscanning data is pooled, forming an extended hyper-brain data matrix. Specifically, suppose that a hyperscanning study involved M groups of participants. In every group, N participants interacted with each other (Fig. 1(A)). For each participant, K channels of fNIRS signals were recorded. The fNIRS data length of the ith group was T_i ($i = 1, 2, \ldots, M$). Then we pool the data as follows (Fig. 1(B)). First, pool all the participants' signals in every group to form its hyper-brain data (i.e., the columns in Fig. 1(B)). Second, concatenate the hyper-brain data of all M groups channel by channel, forming an extended hyper-brain data. Note that if the group members have different social interaction roles according to the experimental design (e.g., teacher and student in a tutorial scene), the

Biomedical Optics EXPRESS

participants of the same role from all groups should be concatenated (i.e., to be put in the same row in Fig. 1(B)). Use $\mathbf{X}_{ij}$ ($i = 1, 2, \ldots, N$; $j = 1, 2, \ldots, M$) to represent the fNIRS data of the ith participant from the jth group, whose dimension is K by T_i. After data pooling, we get the extended hyper-brain data matrix

$$\mathbf{X} = \begin{bmatrix} \mathbf{X}_{11} & \mathbf{X}_{12} & \cdots & \mathbf{X}_{1M} \\ \mathbf{X}_{21} & \mathbf{X}_{22} & \cdots & \mathbf{X}_{2M} \\ \vdots & \vdots & \ddots & \vdots \\ \mathbf{X}_{N1} & \mathbf{X}_{N2} & \cdots & \mathbf{X}_{NM} \end{bmatrix} \tag{1}$$

whose dimension is $N \cdot K$ by $\sum_{i=1}^{M} T_i$. Matrix $\mathbf{X}$ will be ICA-decomposed in the next step.

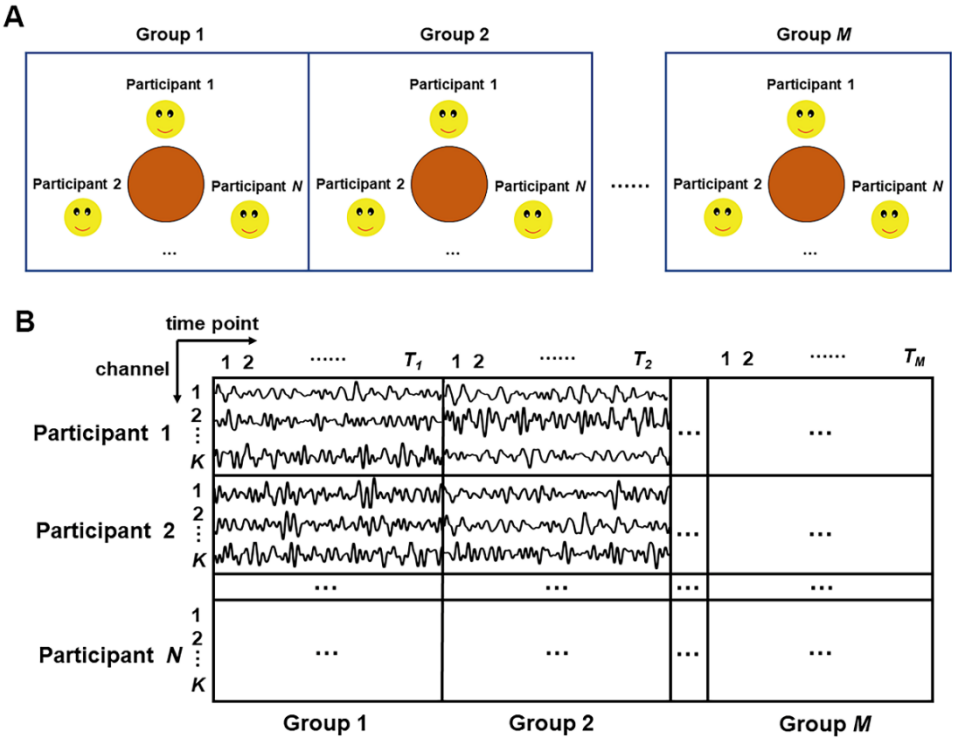

Fig. 1. Data pooling procedure. (A) Participants in each group interact with each other. (B) fNIRS data of all interacting participants in each group are concatenated spatially (i.e., the columns). Data of all groups are concatenated temporally (i.e., the rows). K is the number of channels in each participant. M is the number of groups. T represents the length of time points of single-subject fNIRS data.

2.2. ICA theory

A typical ICA algorithm estimates the linear mixture forward model

$$\mathbf{X} = \mathbf{AS} \tag{2}$$

to obtain $\hat{\mathbf{S}}$ and $\hat{\mathbf{A}}$. For the sake of conciseness, a brief introduction of the ICA theory can be found in Appendix.

Biomedical Optics EXPRESS

2.3. Hyper-brain data decomposition

The hyper-brain data decomposition consisted of two steps. First, the extended hyper-brain data matrix $\mathbf{X}$ (Eq. (1)) is ICA decomposed to obtain $\hat{\mathbf{S}}$ and $\hat{\mathbf{A}}$. For the estimated mixing matrix $\hat{\mathbf{A}}$, of which the dimension is $N \cdot K$ by $N \cdot K$, the columns can be viewed as a set of public spatial modes derived from all the participant groups (similar to the *group-level* results in the single-brain ICA methods).

Second, if we want to obtain the spatial modes and the corresponding time courses of a specific participant group (similar to the *individual-level* results in the single-brain ICA methods), we can use the dual-regression approach [28]. The idea of the dual-regression technique is to apply the estimated public mixing matrix $\hat{\mathbf{A}}$ to every participant group's forward mixing model:

$$\mathbf{X}_j = \mathbf{A}_j \mathbf{S}_j \tag{3}$$

According to Eq. (3), for every participant group j ($j = 1, 2, \ldots, M$), the pooled observed fNIRS signals of all the participants $\mathbf{X}_j$ are a linear combination of a set of source signal $\mathbf{S}_j$. For every j, let $\mathbf{A}_j = \hat{\mathbf{A}}$, then $\mathbf{S}_j$ can be simply estimated by calculating the least-squares solution of Eq. (3):

$$\hat{\mathbf{S}}_j = (\hat{\mathbf{A}}^T \hat{\mathbf{A}})^{-1} \hat{\mathbf{A}}^T \mathbf{X}_j \tag{4}$$

The superscript T means matrix transpose. After $\hat{\mathbf{S}}_j$ is obtained, the group-specific mixing matrix $\mathbf{A}_j$ can be estimated by re-solving Eq. (3):

$$\hat{\mathbf{A}}_j = \mathbf{X}_j \hat{\mathbf{S}}_j^T (\hat{\mathbf{S}}_j \hat{\mathbf{S}}_j^T)^{-1} \tag{5}$$

2.4. Components of interest identification

Similar to the single-brain ICA method, the components of interest can be manually identified according to the spatial pattern or temporal profile. If the brain regions contained in the inter-brain network can be determined based on the research hypothesis and prior knowledge, its related component can also be automatically identified by calculating the goodness of fit (GOF) index between the spatial pattern of the components and the pre-defined spatial template. The GOF index is computed as in Eq. (6):

$$GOF = Z_{in} - Z_{out} \tag{6}$$

where Z_{in} and Z_{out} are the average Z scores of all the channels in a component's spatial pattern falling within and without the template, respectively. The component with the maximum GOF can be identified as the components of interest.

3. Experiments

3.1. Simulation experiment with synthesized data

To validate our method, we simulated an fNIRS dataset of two-person social interaction [29]. Specifically, as shown in Fig. 2(A), we simulated a 40-channel fNIRS measurement (5 rows by 8 columns) on the head surface of each participant in the dyad. The measurement contained two ROIs (regions of interest), simulating two inter-brain networks. The two ROIs consisted of 5 channels and 6 channels, respectively. For each participant we used the MATLAB software to generate 300 s fNIRS data, with a sampling rate of 10 Hz. The data was a mixture of simulated source neural activity and simulated noises. The simulated source neural activity existed only in the ROI channels, and was same in the two participants of the dyad to simulate the brain-to-brain synchronization. The time course of the source neural activity was generated by convolving randomly generated 120 pulsations with the hemodynamic response function (HRF) (Fig. 2(B)). Then all the channels were filled with simulated physiological noise consisting of multiple

Biomedical Optics EXPRESS

sinusoidal signals of different frequencies, including the heartbeat (around 1.1 Hz), the respiration (around 0.25 Hz), the Mayer waves (around 0.1 Hz), and the low-frequency oscillations (0.05 Hz – 0.15 HZ). The amplitude ratio of the neural signal and the physiological noise was set to 2:1. We simulated 60 dyads in total. The simulated neural activity was different across dyads.

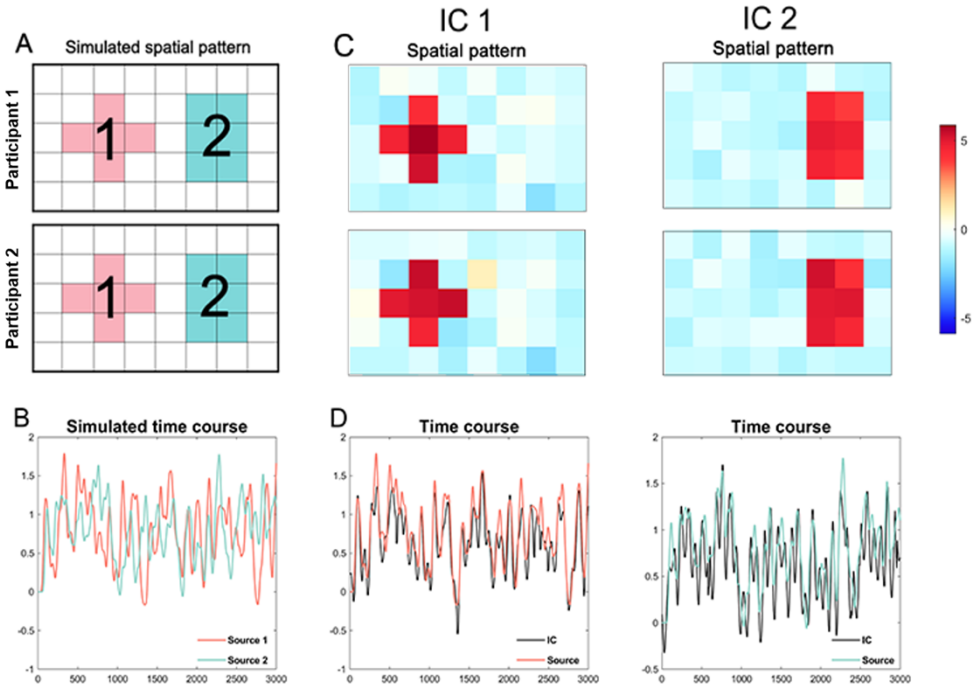

Fig. 2. The simulation experiment and results. (A) The simulated 40-channel fNIRS measurement (5 rows by 8 columns) for each participant in a dyad. The numbered shade areas are the two different ROIs. (B) The time courses of the two simulated neural signals. (C) The spatial patterns of the two decomposed independent components that had the maximum GOF index with the simulated ROI patterns. (D) The time courses of the two decomposed independent components (the black lines) and the corresponding simulated source neural signals (the color lines).

After the data generation, we used the proposed HB-ICA method to decompose the data. Then we compared the decomposed components with the ground truth for validation. Moreover, we also applied the WTC method to the data, and compared the results with the HB-ICA method for validation. Specifically, for WTC analysis, we first used two different filtering methods for preprocessing to remove the physiological noise in the data. One is the conventional bandstop filtering to remove the above-mentioned noise frequency. The other is the wavelet-based method for global physiological noise removal [30]. Then we chose a seed channel in each of the two ROIs (the central channel in ROI 1, and the left-middle channel in ROI 2), respectively. For each ROI, we calculated the WTC between the seed channel's time course and every other channel's time course of the dyad. The WTC values were time and frequency averaged to obtain the IBS. We compared performance of the ICs derived from HB-ICA and the IBS maps derived from WTC in detecting the predefined ROIs by using the receiver operating characteristic (ROC) curve and the area under the ROC curve (AUC) [31].

Biomedical Optics EXPRESS

3.2. Real experiment with in-vivo data

We also applied HB-ICA to an in-vivo hyperscanning dataset from a real social interaction experiment. In the experiment, two college students sat face-to-face and were given a controversial topic close to daily life. They need to discuss the topic and try to reach a consensus. The discussion lasted between 5 to 10 minutes, depending on their discussion progress. Fifty-four participants (21.5 ± 1.9 years of age, 24 males and 30 females), randomly assigned into twenty-seven dyads, were involved in the experiment. Written informed consent was obtained from all the participants prior to the experiments. The experiment protocol was approved by the Institutional Review Board of Shenzhen University.

During the discussion, the two participants' hyperscanning data were acquired by using a NIRScout continuous wave fNIRS system (NIRx Medical Technologies, USA). This apparatus uses two NIR wavelengths (785 nm and 830 nm). The sampling rate was 7.8125 Hz. Two sets of optode patches (one was placed over the prefrontal cortex and the other over the right temporal-parietal cortex) were used to cover the social interaction-related brain regions [32]. These probe sets consisted of 12 laser sources and 11 detectors, forming 32 measurement channels for each of the two participants. The prefrontal patch was placed by approximately putting its bottom middle optode on Fpz of the International 10-20 System [33], and the right temporal-parietal patch was placed by approximately putting its anterior inferior optode on T8. The source-to-detector distance was 3 cm. The cortex localizations of all the channels were obtained by using a 3-dimensional digitizer and the NIRS-SPM software [34] (Fig. 4(A) and (B)).

For pre-processing, the optical density changes were converted to oxygenated hemoglobin (HbO) and deoxygenated hemoglobin (HbR) signals via the modified Beer-Lambert law [35], with the differential pathlength factor of 7.25 and 6.38 for 785 nm and 830 nm, respectively [36]. The first 15 seconds and last 15 seconds of data were discarded to ensure signal stability. The signals were detrended linearly and bilinearly before further analysis.

After pre-processing, the data was analyzed by using the proposed HB-ICA approach. Specifically, first, the data of all the dyads were pooled into the extended hyper-brain data matrix. The sequence of the two participants in a dyad was randomly assigned because they had equal positions and roles in the interaction. Second, the extended hyper-brain data matrix was ICA decomposed with the TDSEP algorithm, and the public mixing matrix $\hat{\mathbf{A}}$ was obtained. Third, the dyad-specific spatial modes $\hat{\mathbf{A}}_j$ and the corresponding time courses $\hat{\boldsymbol{S}}_j$ of every dyad j was obtained by using the dual-regression method.

Previous studies suggested that the right dorsal lateral prefrontal cortex (r-DLPFC) and the right temporal-parietal junction (r-TPJ) are involved in social interaction activities [37–39]. Therefore, to identify the social interaction-related multi-brain network, we defined two spatial templates by using the anatomical localization information. One contained both participants' right DLPFC areas as ROI. The other contained both participants' right TPJ areas as ROI. (Figure 4(C) and (D)). The components whose spatial pattern has the highest GOF index with the templates were identified.

4. Results

4.1. Results of the simulation experiment with synthesized data

For the simulation experiment, Fig. 2(C) and (D) illustrated the spatial patterns and the time courses of the two independent components identified by the HB-ICA method, respectively. The left column of Fig. 2(C) and (D) showed one component (IC 1) of which the spatial pattern was the most similar with the ROI 1 (GOF = 2.89). The Pearson's correlation coefficient between the time course of IC 1 (the black curve) and the ground truth source signal (the red curve) was 0.86. The right column of Fig. 2(C) and (D) showed another component (IC 2) of which the spatial pattern was the most similar with the ROI 2 (GOF = 2.74). The Pearson's correlation coefficient

Biomedical Optics EXPRESS

between the time course of IC 2 (the black curve) and the ground truth source signal (the green curve) was 0.91.

Figure 3 showed the comparison results between HB-ICA and WTC analysis with the synthesized data. The first row of Fig. 3(A) showed the spatial patterns of the two ROI components found by HB-ICA. In comparison, the second and the third row of Fig. 3(A) showed the group averaged WTC maps derived from the seed channel-based WTC analysis, preprocessed with the bandstop filtering and the wavelet-based filtering, respectively. All these spatial patterns successfully identified the predefined ROIs by presenting apparent contrast between the ROI and non-ROI areas. However, within the non-ROI areas, the WTC maps also showed positive coherence with the seed channel. This is due to the residual global noise, and the wavelet-based filtering showed better noise removal ability than the bandstop filtering. Figure 3(B) showed the ROC curves of the three analysis methods. The red, blue and green lines illustrated the HB-ICA, WTC with wavelet-based filtering and WTC with bandstop filtering, respectively, and the area under curve (AUC) indices were 0.92, 0.89 and 0.79, respectively.

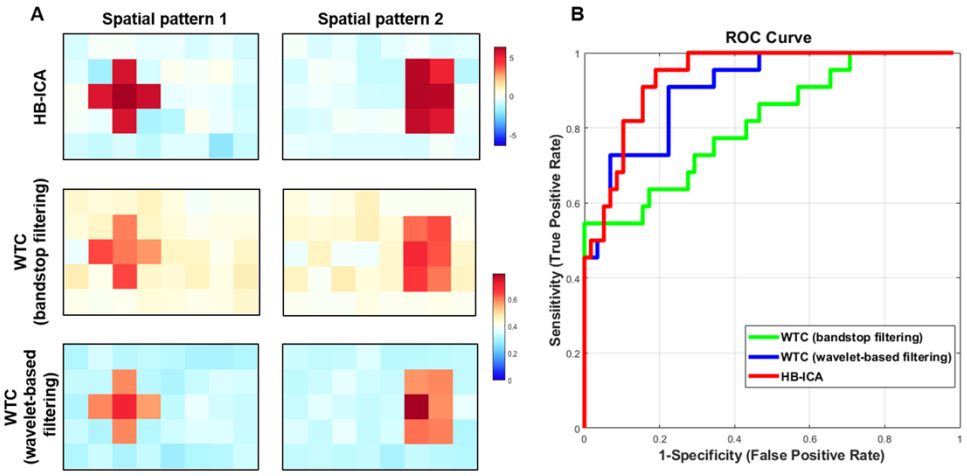

Fig. 3. Comparison results between the HB-ICA and the WTC method with the synthesized data. (A) The spatial patterns derived from different methods. (B) The ROC curves of different methods.

4.2. Results of the real experiment results with in-vivo data

Figure 4 showed the results of the real experiment results with in-vivo fNIRS data. First, according to the fNIRS measurement localization results (Fig. 4(A) and (B)), we identified two spatial templates (r-DLPFC and r-TPJ, as shown in Fig. 4(C) and (D)). Then we applied the proposed HB-ICA approach to the HbO data to obtain the independent components (IC), and obtained 64 ICs in total. Finally, we used the GOF index to evaluate the similarity between the two spatial templates and all the spatial patterns of these independent components. Figure 4(E) showed the spatial pattern of the IC that had the maximum GOF index with the r-DLPFC template (GOF = 1.82), and Fig. 4(F) showed the spatial pattern of the IC that had the maximum GOF index with the r-TPJ template (GOF = 1.25).

Biomedical Optics EXPRESS

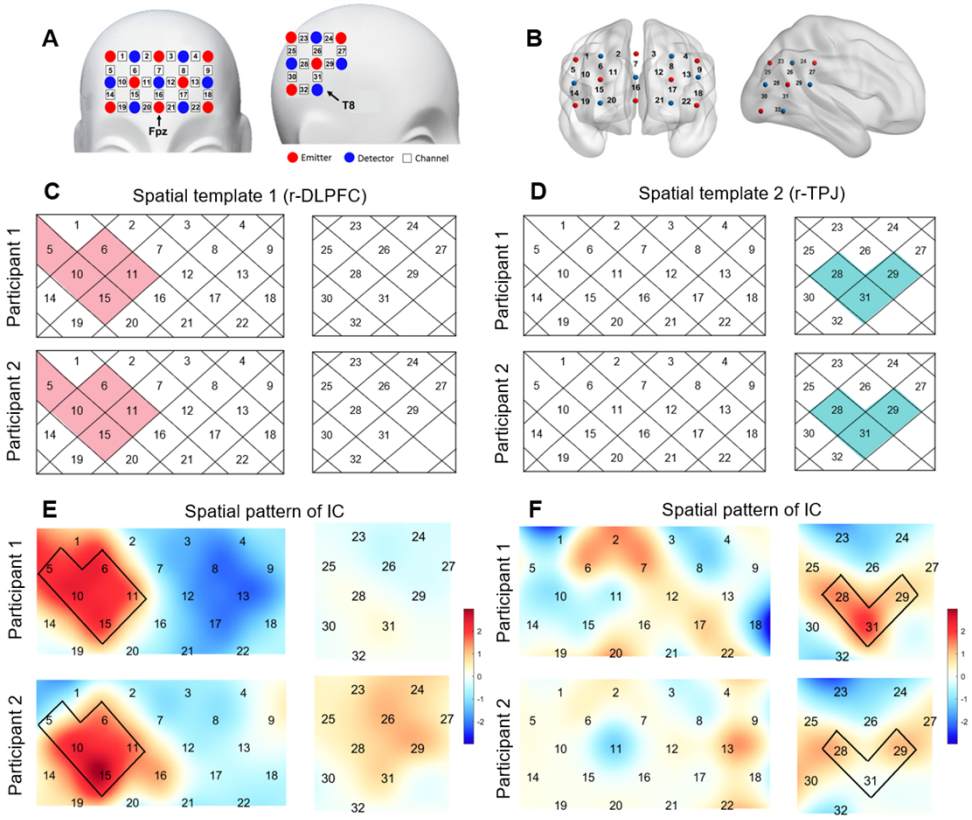

Fig. 4. The in-vivo experiment and results. (A) The fNIRS optodes and channels arrangement. (B) The cortical localization of the fNIRS channels. (C) The spatial template contained the ROI of the r-DLPFC. (D) The spatial template contained the ROI of the r-TPJ. (E) The spatial pattern of the decomposed independent component that had the maximum GOF index with the r-DLPFC template (the black frame). (F) The spatial pattern of the decomposed independent component that had the maximum GOF index with the r-TPJ template (the black frame).

5. Discussion

In the present study, we introduced the HB-ICA method to calculate the inter-brain networks for fNIRS-hyperscanning studies. To validate this new approach, we conducted both simulation and in vivo fNIRS experiments. In the simulation experiment, the HB-ICA showed good performance by finding components that were highly consistent with the ground truth inter-brain networks in both spatial pattern and time course (Fig. 2). The comparison between the HB-ICA and seed-based WTC showed high consistency between the two methods in identifying the inter-brain network. Moreover, by using the in-vivo fNIRS-hyperscanning data, the HB-ICA method successfully found two inter-brain networks (i.e., the dual r-DLPFC network and the dual r-TPJ network) reported in previous hyperscanning studies [37–39] (Fig. 4). Taken together, these results suggested that the HB-ICA method is quite effective for inter-brain network detection.

The HB-ICA is a fully data-driven method. It finds statistically independent components from the hyper-brain data instead of calculating the inter-brain synchronization. This essential property endowed the HB-ICA with several advantages. First, it doesn't need to specify any frequency parameters about the inter-brain networks. In traditional WTC-based hyperscanning studies,

Biomedical Optics EXPRESS

researchers needed to assume the frequency characteristics of the inter-brain synchronization, which heavily relies on experience and previous literatures. Since the frequency characteristics of the inter-brain information communication may differ among different social interaction tasks, it would reduce the sensitivity and specificity in detecting the inter-brain synchronization if the frequency band had not been properly specified. Second, HB-ICA look for inter-brain networks in a multi-variate way. It utilizes all the fNIRS channels simultaneously and can obtain the inter-brain networks composed of multiple brain regions. Therefore, the HB-ICA method provides a way to study the inter-brain information communication from a perspective of inter-brain network. In comparison, the WTC-based IBS calculation is a univariate method. It one-by-one evaluates and tests the inter-brain synchronization between two channels that respectively come from different participants of a dyad, and thus may neglect the relationship between these point-to-point synchronizations. Third, the HB-ICA method proved to be insensitive to the global physiological noise in fNIRS signals. The global physiological noise removal is usually a difficult problem in fNIRS, and requires additional hardware support (e.g., short source-detector distance channels or ultrasound Doppler sensors) or noise removal algorithms [30]. However, our results suggested that the HB-ICA method could robustly find the inter-brain networks even if no global physiological noise removal was applied (as shown in Fig. 3). This is mainly because ICA can separate fNIRS global physiological noise [26] as independent components and thus can bring great convenience for researchers.

The present study has also some limitations that can be improved in future works. For example, the current components of interest identification procedure mainly used the spatial pattern information of the components. In the future, we will further investigate the relationship between the time course of the independent components and the social interaction behaviors, and explore new component identification method based on integrated temporal and spatial information. Moreover, in the hyper-brain data decomposition procedure, we will further try different ICA algorithms (e.g., the FastICA [40]) to optimize the performance. In addition, in the present study, we did not conduct quantitative comparison between the HB-ICA and the traditional WTC method with in-vivo data. This is mainly because hyperscanning research is still a quite new area at present, and it is difficult to acquire sufficiently effective experiment paradigm and accurate ground truth to serve as the benchmark. In the future, it is also important to apply the HB-ICA approach to various of social interaction paradigms and to further compare its performance with other methods.

In summary, the present study proposed a new inter-brain network detection approach (HB-ICA) for fNIRS-hyperscanning studies, and validated its effectiveness by using both simulated data and in vivo data. The HB-ICA method can be complementary to the traditional WTC-based methods for INS calculation, and can further be applied to investigate the multi-brain networks of groups containing more than two participants. This new approach provides a promising way to analyzing the fNIRS-hyperscanning data, and will bring new insights to the neural mechanism studies on human social interactions.

Appendix

A typical ICA model assumes that a set of observed signals are the linear mixture of a set of statistically independent and non-Gaussian source signals [41]. That is

$$\mathbf{X} = \mathbf{AS} \tag{A.1}$$

where $\mathbf{X}$ is the observed mixture signal matrix (a row is a signal, while a column is a time point). $\mathbf{S}$ is the source signal matrix. $\mathbf{A}$ is called the mixing matrix. The target is to recover $\mathbf{S}$ from $\mathbf{X}$, under the condition that $\mathbf{A}$ is unknown (known as the blind source separation problem). An ICA

Biomedical Optics EXPRESS

algorithm can give a set of estimations to the source signals expressed by

$$\hat{\mathbf{S}} = \mathbf{WX} \tag{A.2}$$

where $\hat{\mathbf{S}}$ is the estimated source signal matrix, and $\mathbf{W}$ is called the unmixing matrix. The pseudoinverse matrix of the unmixing matrix $\mathbf{W}$ can be viewed as an approximation to the mixing matrix $\mathbf{A}$:

$$\hat{\mathbf{A}} = \mathbf{W}^{-} \tag{A.3}$$

In equation (A.1), the elements of the kth column of $\mathbf{A}$ give the weights with whom the source signals in $\mathbf{S}$ are mixed to form the kth mixture signal in $\mathbf{X}$. When using ICA to decompose the fNIRS data, we usually take measurement channels as variables and take time points as samples, which is called the temporal ICA [42,43]. Therefore, in fNIRS, we can view the columns of $\hat{\mathbf{A}}$ as a set of the spatial modes, and view the rows of $\hat{\mathbf{S}}$ as a set of the temporal activities related to these spatial modes.

There are various algorithms for ICA decomposition (e.g., the FastICA [40]). These algorithms usually have different assumptions and optimization functions and have different performances in specific situations. In the present study, we adopted the temporal decorrelation source separation algorithm (TDSEP) [44] to conduct the ICA decomposition. The reason is that the fNIRS signal is usually temporally autocorrelated due to its high sampling rate and has complicated noise characteristics [45], and it was suggested that the TDSEP may have better performance than other algorithms when the source signal has significant temporal autocorrelation structure [46] and low signal-to-noise ratio [47]. Moreover, compared with other algorithms, the TDSEP is more tolerant when the non-Gaussian assumption is strictly satisfied [46].

Funding. National Natural Science Foundation of China (32071072); Shenzhen-Hong Kong Institute of Brain Science (2023SHIBS0004); Shenzhen Science and Technology Innovation Program (JCYJ20210324093208021).

Disclosures. The authors declare no conflicts of interest.

Data availability. Data underlying the results presented in this paper are not publicly available at this time but may be obtained from the authors upon reasonable request.

References

1. A. Pérez, M. Carreiras, J. A. Duñabeitia, *et al.*, "Brain-to-brain entrainment: EEG interbrain synchronization while speaking and listening," Sci. Rep. **7**(1), 4190 (2017).
2. U. Lindenberger, S.-C. Li, W. Gruber, *et al.*, "Brains swinging in concert: cortical phase synchronization while playing guitar," BMC Neurosci. **10**(1), 22 (2009).
3. A. Pérez, G. Dumas, M. Karadag, *et al.*, "Differential brain-to-brain entrainment while speaking and listening in native and foreign languages," Cortex **111**, 303–315 (2019).
4. Y. Pan, S. Dikker, P. Goldstein, *et al.*, "Instructor-learner brain coupling discriminates between instructional approaches and predicts learning," NeuroImage **211**, 116657 (2020).
5. N. Liu, C. Mok, E. E. Witt, *et al.*, "NIRS-based hyperscanning reveals inter-brain neural synchronization during cooperative jenga game with face-to-face communication," Front. Hum. Neurosci. **10**, 82 (2016).
6. I. Davidesco, E. Laurent, H. Valk, *et al.*, "The temporal dynamics of brain-to-brain synchrony between students and teachers predict learning outcomes," Psychol. Sci **34**(5), 633 (2023).
7. P. Montague, G. S. Berns, J. D. Cohen, *et al.*, "Hyperscanning: Simultaneous fMRI during Linked Social Interactions," NeuroImage **16**(4), 1159–1164 (2002).
8. X. Cui, D. M. Bryant, A. L. Reiss, *et al.*, "NIRS-based hyperscanning reveals increased interpersonal coherence in superior frontal cortex during cooperation," NeuroImage **59**(3), 2430–2437 (2012).
9. A. P. Key, Y. Yan, M. Metelko, *et al.*, "Greater social competence is associated with higher interpersonal neural synchrony in adolescents with autism," Front. Hum. Neurosci. **15**, 790085 (2022).
10. H. Tanabe, H. Kosaka, D. N. Saito, *et al.*, "Hard to "tune in": neural mechanisms of live face-to-face interaction with high-functioning autistic spectrum disorder," Front. Hum. Neurosci. **6**, 268 (2012).
11. X. Deng, X. Chen, L. Zhang, *et al.*, "Adolescent social anxiety undermines adolescent-parent interbrain synchrony during emotional processing: A hyperscanning study," International Journal of Clinical and Health Psychology **22**(3), 100329 (2022).
12. M. A. Saul, X. He, S. Black, *et al.*, "A two-person neuroscience approach for social anxiety: a paradigm with interbrain synchrony and neurofeedback," Front. Psychol. **12**, 568921 (2022).

Biomedical Optics EXPRESS

13. R. Li, N. Mayseless, S. Balters, *et al.*, "Dynamic inter-brain synchrony in real-life inter-personal cooperation: A functional near-infrared spectroscopy hyperscanning study," NeuroImage **238**, 118263 (2021).
14. Y. Zhang, W. Ye, J. Yin, *et al.*, "Exploring the role of mutual prediction in inter-brain synchronization during competitive interactions: an fNIRS hyperscanning investigation," Cereb. Cortex **34**(1), 483 (2024).
15. S. Dikker, L. Wan, I. Davidesco, *et al.*, "Brain-to-brain synchrony tracks real-world dynamic group interactions in the classroom," Curr. Biol. **27**(9), 1375–1380 (2017).
16. S. Kinreich, A. Djalovski, L. Kraus, *et al.*, "Brain-to-brain synchrony during naturalistic social interactions," Sci. Rep. **7**(1), 17060 (2017).
17. A. Czeszumski, S. H.-Y. Liang, S. Dikker, *et al.*, "Cooperative behavior evokes interbrain synchrony in the prefrontal and temporoparietal cortex: a systematic review and meta-analysis of fNIRS hyperscanning studies," eNeuro **9**(2), 0268 (2022).
18. B. Dai, C. Chen, Y. Long, *et al.*, "Neural mechanisms for selectively tuning in to the target speaker in a naturalistic noisy situation," Nat. Commun. **9**(1), 2405 (2018).
19. T. Nozawa, Y. Sasaki, K. Sakaki, *et al.*, "Interpersonal frontopolar neural synchronization in group communication: An exploration toward fNIRS hyperscanning of natural interactions," NeuroImage **133**, 484–497 (2016).
20. Y. Liu, E. A. Piazza, E. Simony, *et al.*, "Measuring speaker-listener neural coupling with functional near infrared spectroscopy," Sci. Rep. **7**(1), 43293 (2017).
21. L. Duan, R.-N. Dai, X. Xiao, *et al.*, "Cluster imaging of multi-brain networks (CIMBN): a general framework for hyperscanning and modeling a group of interacting brains," Front. Neurosci. **9**, 267 (2015).
22. T. Liu, L. Duan, R. Dai, *et al.*, "Team-work, Team-brain: Exploring synchrony and team interdependence in a nine-person drumming task via multiparticipant hyperscanning and inter-brain network topology with fNIRS," NeuroImage **237**, 118147 (2021).
23. J. Yang, H. Zhang, J. Ni, *et al.*, "Within-group synchronization in the prefrontal cortex associates with intergroup conflict," Nat. Neurosci. **23**(6), 754–760 (2020).
24. S. Dikker, L. J. Silbert, U. Hasson, *et al.*, "On the same wavelength: Predictable language enhances speaker–listener brain-to-brain synchrony in posterior superior tempora l gyrus," J. Neurosci. **34**(18), 6267–6272 (2014).
25. E. A. Allen, E. Damaraju, S. M. Plis, *et al.*, "Tracking whole-brain connectivity dynamics in the resting state," Cereb. Cortex **24**(3), 663–676 (2014).
26. H. Zhang, Y.-J. Zhang, C.-M. Lu, *et al.*, "Functional connectivity as revealed by independent component analysis of resting-state fNIRS measurements," NeuroImage **51**(3), 1150–1161 (2010).
27. H. Zhang, L. Duan, Y.-J. Zhang, *et al.*, "Test-retest assessment of independent component analysis-derived resting-state functional connectivity based on functional near-infrared spectroscopy," NeuroImage **55**(2), 607–615 (2011).
28. C. F. Beckmann, C. Mackay, N Filippini, *et al.*, "Group comparison of resting-state FMRI data using multi-subject ICA and dual regression," NeuroImage **47**, S148 (2009).
29. Y. Zhao, R.-N. Dai, X. Xiao, *et al.*, "Independent component analysis-based source-level hyperlink analysis for two-person neuroscience studies," J. Biomed. Opt. **22**(2), 027004 (2017).
30. L. Duan, Z. Zhao, Y. Lin, *et al.*, "Wavelet-based method for removing global physiological noise in functional near-infrared spectroscopy," Biomed. Opt. Express **9**(8), 3805 (2018).
31. L. Duan, Y.-J. Zhang, C.-Z. Zhu, *et al.*, "Quantitative comparison of resting-state functional connectivity derived from fNIRS and fMRI: A simultaneous recording study," NeuroImage **60**(4), 2008–2018 (2012).
32. R. Saxe, "Uniquely human social cognition," Curr. Opin. Neurobiol. **16**(2), 235–239 (2006).
33. H. H. Jasper, "The 10–20 electrode system of the International Federation," Electroencephalogr. Clin. Neurophysiol. **10**, 370–375 (1958).
34. J. C. Ye, S Tak, K Jang, *et al.*, "NIRS-SPM: Statistical parametric mapping for near-infrared spectroscopy," NeuroImage **44**(2), 428–447 (2009).
35. M. Cope and D. T. Delpy, "System for long-term measurement of cerebral blood and tissue oxygenation on newborn infants by near infra-red transillumination," Med. Biol. Eng. Comput. **26**(3), 289–294 (1988).
36. M. Hiraoka, M Firbank, M Essenpreis, *et al.*, "A Monte Carlo investigation of optical pathlength in inhomogeneous tissue and its application to near-infrared spectroscopy," Phys. Med. Biol. **38**(12), 1859–1876 (1993).
37. E. Bilek, M. Ruf, A. Schäfer, *et al.*, "Information flow between interacting human brains: Identification, validation, and relationship to social expertise," *Proc. Natl. Acad. Sci. U. S. A.* (2015).
38. G. J. Stephens, L. J. Silbert, U. Hasson, *et al.*, "Speaker-listener neural coupling underlies successful communication," Proc. Natl. Acad. Sci. **107**(32), 14425–14430 (2010).
39. Z. Zada, S. Nastase, A. Goldstein, *et al.*, "Brain-to-brain linguistic coupling in natural conversations," *2022 Conference on Cognitive Computational Neuroscience* (2022).
40. A. Hyvärinen, "Fast and robust fixed-point algorithms for independent component analysis," IEEE Trans. Neural Netw. **10**(3), 626–634 (1999).
41. P. Comon, "Independent component analysis, A new concept?" Signal Processing **36**(3), 287–314 (1994).
42. K. Satoru, I. Miyai, A. Seiyama, *et al.*, "Removal of the skin blood flow artifact in functional near-infrared spectroscopic imaging data through independent component analysis," J. Biomed. Opt. **12**(6), 062111 (2007).
43. J. Markham, B. R. White, B. W. Zeff, *et al.*, "Blind identification of evoked human brain activity with independent component analysis of optical data," Human brain mapping **30**(8), 2382–2392 (2009).

Biomedical Optics EXPRESS

44. A. Ziehe and K.-R. Müller, "TDSEP — an efficient algorithm for blind separation using time structure," in *ICANN 98*, (Springer, 1998), 675–680.
45. J. Barker, A. Aarabi, T. J. Huppert, *et al.*, "Autoregressive model based algorithm for correcting motion and serially correlated errors in fNIRS," Biomed. Opt. Express **4**(8), 1366–1379 (2013).
46. N. Nicolaou and S. J. Nasuto, "Comparison of Temporal and Standard Independent Component Analysis (ICA) Algorithms for EEG Analysis," in *ICANN/ICONIP*, volume 3 (2003).
47. G. R. Naik, D. K. Kumar, H. Weghorn, *et al.*, "Subtle hand gesture identification for HCI using temporal decorrelation source separation BSS of surface EMG," in *9th Biennial Conference of the Australian Pattern Recognition Society on Digital Image Computing Techniques and Applications (DICTA 2007)*, 30–37 (2007).